J Polym Res (2014) 21:416
DOI 10.1007/s10965-014-0416-5

ORIGINAL PAPER

Electrodeposition of polyaniline-montmorrilonite nanocomposite coatings on 316L stainless steel for corrosion prevention

Mehdi Shabani-Nooshabadi · Sayed Mehdi Ghoreishi · Yaser Jafari · Naser Kashanizadeh

Received: 24 November 2013 / Accepted: 6 March 2014

Abstract The synthesis of polyaniline- montmorrilonite (MMT) nanocomposite coatings on 316L stainless steel (316L SS) surface has been investigated by using the galvanostatic method. The synthesized coatings were characterized by Fourier Transform Infrared Spectroscopy (FT-IR), UV-visible absorption spectrometry and Scanning Electron Microscopy (SEM). The anticorrosion performances of polyaniline-MMT nanocomposite coatings were investigated in 0.5 M HCl medium by the potentiodynamic polarization technique and Electrochemical Impedance Spectroscopy (EIS). The corrosion rate of polyaniline-MMT nanocomposite coated 316L SS was found ~540 times lower than bare 316L SS and potential corrosion increased from −0.386 V versus Ag/AgCl for uncoated 316L SS to −0.040 V versus Ag/AgCl for polyaniline-MMT nanocomposite coated 316L SS electrodes. Electrochemical measurements indicate that polyaniline-MMT nanocomposite coated have good inhibiting properties with mean efficiency of ~99.8 % at 0.75 mA cm^{-2} current density applied on 316L SS corrosion in acid media. The results of this study clearly ascertain that the polyaniline-MMT nanocomposite has an outstanding potential to protect 316L SS against corrosion in an acidic environment.

Keywords Polyaniline- montmorrilonite · Coating · 316L stainless steel · Corrosion

M. Shabani-Nooshabadi (✉) · S. M. Ghoreishi · Y. Jafari · N. Kashanizadeh
Department of Analytical Chemistry, Faculty of Chemistry, University of Kashan, Kashan, Iran
e-mail: m.shabani@kashanu.ac.ir

Published online: 30 March 2014

Introduction

Iron and its alloys are widely used in many applications and diversity of these applications were intensified the researches relating to enhancement of corrosion resistance of iron based metals in various neutral or aggressive environments [1–7] Type 316L stainless steel (316L SS) belong to a class of metals and alloys that are protected by a passive film formed on their surface. However, these alloys are susceptible to localised attack; even high alloyed steels may corrode in strong chloride solutions. The localised corrosion of 316L SS is one of the most serious problems facing the use of these alloys [8]. This localized attack is an especially important limitation of the material for biomedical applications [9, 10]. The release of metal ions such as iron, chromium and nickel in the biological environment surrounding the alloy results in a decreased biocompatibility. Several strategies have been used to generate more protective interfaces on stainless steels, including the use of conducting polymers [11–13].

Conductive polymers continue to be of considerable interest as components of corrosion resistant coatings. Passivation of stainless steels is typically achieved by chemically or electrochemically coating the surface with such conductive polymers. The polymer film passivates the electrode by holding the potential in the passive region [14–21]. Among conducting polymers, polyaniline and polypyrrole are a potential material for various commercial applications that has been studied more than other conducting polymers because of its high electrical conductivity, environmental stability, ease of preparation in large quantities and relatively low cost [22–25].

There has been a lot of interest lately in the use of conducting polymers such as polyaniline [26, 27] and polypyrrole [28, 29] obtained by electrodeposition as anticorrosion coatings for prevention of stainless steel corrosion in corrosive medium. Hermas et al. [20] reported that polyaniline (PANi) enhanced the passivity of stainless steel

by increasing the Cr_2O_3 content in the passive film and inhibiting the interaction of the oxide with solution. It was also reported that conducting polyaniline coatings on stainless steel inhibited the formation of pitting corrosion. Huh and coworkers [27] have shown that the performance of corrosion protection provided by polyaniline to steel depends on the doping type in the polyaniline and the nature of the corrosion environment. Conducting polymers such as poly(o-methoxyaniline) [15], poly(2,5 dimethoxyaniline)-fluoropolymer blends [30] and poly(m-methoxytoluene) [31] can be also easily electropolymerized on stainless steel surfaces in various electrolytes. These polymers obtained on stainless steel surfaces showed that substituted conducting polymers can be also used as a protective coating against corrosion in neutral and acidic chloride environment.

Several strategies have been used to increase the effectiveness of polyaniline as an anticorrosive coating on metals. The utility of various nanoparticles, such as ones made from inorganic materials [32], natural fibers [33], graphite [34], carbon nanotubes [35, 36] and nano clays (layered silicates) [37–39], as additives to enhance the mechanical and barrier performance of polymers has been established [40]. Polymer/clay nanocomposites have drawn considerable interest over the last decade because of their ability to strengthen the gas barrier as well as improve the thermal stability, mechanical strength and fire-retardant properties of polymers [41–44]. The use of the natural, abundant, inexpensive material montmorillonite (MMT) in the preparation of polymer/clay composites is a significant research topic. MMT has the attractive features of a large surface area, ion-exchange properties [45, 46]. Several studies have shown that the incorporation of MMT into different resins can effectively enhance the corrosion protection performance of resins on metallic surfaces because MMT increases the lengths of the diffusion pathways of oxygen, water and aggressive ions [47, 48].

Recently, the research interests on developing polymer-clay nanocomposite materials have shifted to water-based system due to the concerns on environmental and health issues, but there haven't been reports on the direct electrosynthesis of polyaniline-MMT nanocomposite coatings on a 316L SS electrode. The main objective of the present study is to direct electropolymerize polyaniline and polyaniline- MMT nanocomposite on 316L SS electrode from H_2SO_4 solution via the galvanostatic method by optimizing the electrodeposition conditions. The aqueous electrodeposition process is an environmental friendly and efficient technique used to process conducting polymer coatings. It is widely preferred because of its simplicity and it also can be used as a one-step method to form coatings on metal substrates. It allows efficient control of the chemical and physical properties of the coatings, and it can also be easily adapted to large-scale production [48].

In this work, we have electrochemically synthesized polyaniline and polyaniline-MMT nanocomposite coating on 316L SS by using the direct electrochemical galvanostatic method. The synthesized coatings were characterized by Fourier transform infrared (FT-IR) spectroscopy, UV-visible absorption spectrometry and scanning electron microscopy (SEM). The corrosion resistant properties of the polyaniline and polyaniline-MMT nanocomposite coated samples were then evaluated by Tafel polarization and EIS techniques in 0.5 M HCl solution.

Material and methods

MMT was purchased from Fluka. Other chemicals were purchased from Merck. Aniline was freshly distilled and stored in the dark. All solutions were freshly prepared from analytical grade chemical reagents using doubly distilled water. For each run, a freshly prepared solution and a cleaned set of electrodes were used, and all experiments were carried out at room temperature.

Electrochemical experiments and corrosion tests were carried out using a μ-AUTOLAB potentiostat/galvanostat model μIII AUTO71174 connected to a Pentium IV personal computer through a USB electrochemical interface. Pretreated 316L SS was used as working electrode in the conventional three-electrode cell.

Type 316L SS rods in the form of discs was cut into rectangular samples of 1 cm^2 area, soldered with Cu-wire for an electrical connection and mounted onto the epoxy resin to offer only one active flat surface exposed to the corrosive environment and used as working electrodes. Its chemical composition (wt %) is: 17.47 Cr, 10.32 Ni, 1.88 Mn, 1.90 Mo, 0.39 Si, 0.025C and Fe balance. Before each experiment, the surface pre-treatment of the working electrode was prepared by mechanical abrading of the electrode surface with successive grades of emery papers 1200. The electrode was washed with doubly distilled water, degreased with acetone and ethanol. Following this pretreatment, the electrode was immediately transferred to the electrochemical cell. The auxiliary electrode was a large Pt sheet and an Ag/AgCl (in 3 M KCl) electrode was used as a reference electrode. All the potentials in this work are quoted vs. Ag/AgCl.

As a typical procedure for the preparation of polyaniline-MMT nanocomposite coatings with 1 wt% of MMT clay, an appropriate amount of MMT clay was introduced into 100 mL of distilled water and was magnetically stirred overnight at room temperature. Then, a mixture of 0.5 M of H_2SO_4 and 0.4 M of aniline monomer was added into the clay solution under magnetic stirring for 3 h. Subsequently, the obtained solution was ultrasonicated for 30 min in order to increase its uniformity. Electropolymerization was carried out by galvanostatic polarization from 10 mL of the prepared solution.

Electrosynthesis of polyaniline-MMT coatings over the 316L SS surface were carried out by imposing a fixed current for certain duration of time. In this regard, current densities viz. 0.25, 0.5, 0.75 and 1.00 mA cm^{-2} for duration of time of 500 s and the corresponding potential transients were recorded. After the electropolymerization reaction, the green colored, homogeneous and adherent polyaniline nanocomposite coatings containing MMT were successfully obtained on 316L SS.

The FT-IR spectra of an electrosynthesized polyaniline-MMT nanocomposite over 316L SS was obtained and compared to polyaniline and MMT clay using a Shimadzu Varian 4300 spectrophotometer in KBr pellets. The electrosynthesized polyaniline-MMT nanocomposites were dissolved in pure N-methylpyrrolidone (NMP) and UV–Vis spectra of these polymer solutions were recorded on a Perkin Elmer Lambda2S UV–Vis spectrometer. The morphologies of the electropolymerized coatings on 316L SS were analyzed using a PHILIPS model XL30 scanning electron microscope instrument operating at 10 kV. The samples were mounted on a double-sided adhesive carbon disc and sputtercoated with a thin layer of gold to prevent sample charging problems.

The 316L SS samples with electrosynthesized polyaniline-MMT nanocomposite coatings were evaluated for their corrosion resistance properties in 0.5 M HCl medium by Tafel polarization and electrochemical impedance spectroscopy (EIS). The working electrode was first immersed in the test solution for 30 min to establish a steady state open circuit potential (OCP).

In the case of Tafel polarization, the potential was scanned at ±200 mV versus OCP at a scan rate of 0.005 mV s^{-1}. From the anodic and cathodic polarization curves, the Tafel regions were identified and extrapolated to the corrosion potential (E_{corr}) to obtain the corrosion current (I_{corr}) using the NOVA 1.6. In the case of electrochemical impedance spectroscopy, a.c. signals of 10 mV amplitude and various frequencies from 30 kHz to 0.01 Hz at open circuit potentials were impressed to the coated 316L SS in the electrode surface 1 cm^2. A Pentium IV powered computer and NOVA 1.6 software were applied for analyzing impedance data.

Results and discussion

Electropolymerization

The experiments were performed under galvanostatic conditions. The E-t transient curves were obtained during the formation of polyaniline and polyaniline-MMT nanocomposite coatings on 316L SS for four different applied constant current densities 0.25, 0.50, 0.75 and 1.00 mA cm^{-2} (Fig. 1a and b). Coatings of homogeneous appearance were obtained at all applied current densities. The time to reach the maximum potential value is different for the applied current densities

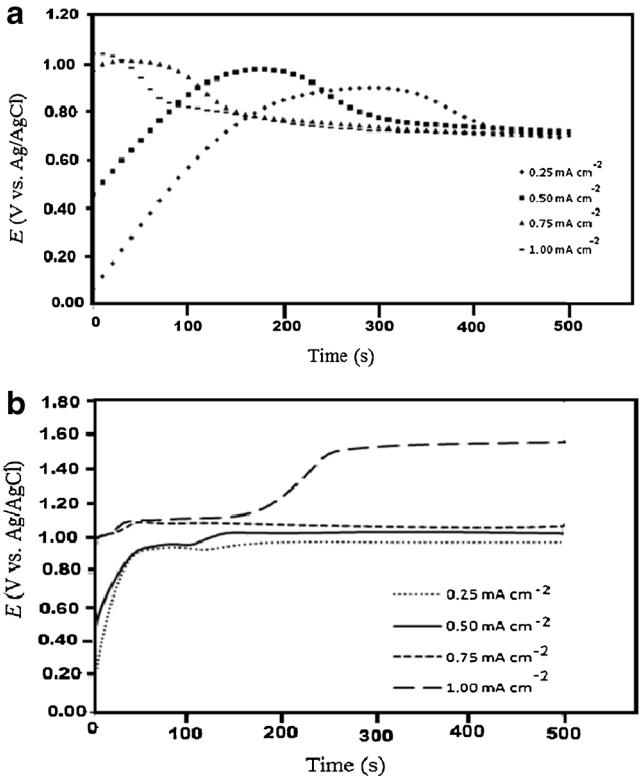

Fig. 1 E-t curves under galvanostatic polymerization conditions in 0.5 M H_2SO_4 solution containing **a** 0.4 M aniline and **b** 0.4 M aniline and 1 wt% dispersed MMT nanoparticles for 316L SS electrode at various current densities (mA cm^{-2})

that it is nominated as induction time. As it can be seen in Fig. 1, in the current density range of 0.25–0.75 mA cm^{-2} the increased of current density is consistent with the decrease of induction time but in current density 1.00 mA cm^{-2}, there is reverse result. Also, less induction time is needed for synthesized of polyaniline-MMT nanocomposite coating comparing to polyaniline. The polyaniline and polyaniline-MMT nanocomposite coatings synthesized by a current density of 0.75 mA cm^{-2} is adhesive and uniform but was not adhesive coatings synthesized at high current density (1.00 mA cm^{-2}) and they are destroyed since washed with ethanol and water. The galvanostatic procedure gave rise to the deposition of a green coating, characteristic of polyaniline and polyaniline-MMT nanocomposite in the emeraldine oxidation state on the surface of 316L SS.

Characterization of polyaniline-MMT nanocomposite films

The representative FT-IR absorption spectra of MMT clay, pure polyaniline and the polyaniline-MMT nanocomposite containing 1 wt% clay are shown in Fig. 2. The peak at 3,260 cm^{-1} representing the secondary amine and 1,512 cm^{-1} and 1,592 cm^{-1} representing the benzenoid and quinoid rings of polyaniline, respectively. The spectrum for the MMT displays

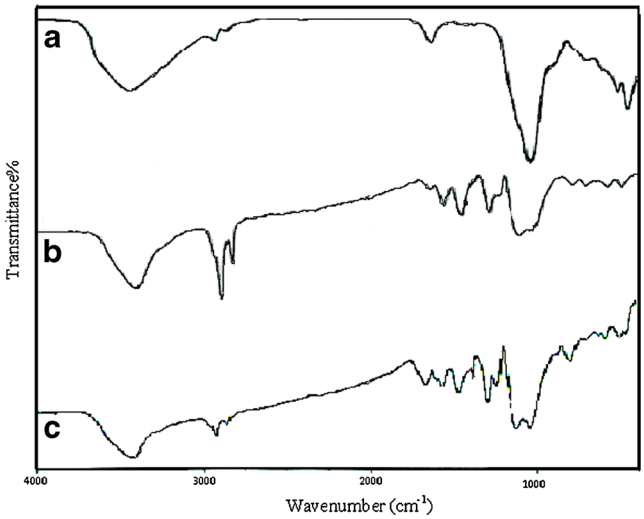

Fig. 2 FT-IR spectra **a** Na^{+}-MMT nanoparticles, **b** polyaniline and **c** the polyaniline-MMT nanocomposite

the usual appearance with a peak at ~1,050 cm^{-1}, representing the Si-O bond stretching and doublet peaks at ~2,920 cm^{-1} and 2,850 cm^{-1} from C-H stretching bond within the MMT structure from the quaternary ammonium modifier [48] and another doublet peaks at 450–600 cm^{-1} are due to Si-O bond bending, Al-O bond stretching and Mg-O. The bands of Al-O bond bending are observed at 918 cm^{-1} and 795 cm^{-1}. The peak at 468 cm^{-1} is representing the Mg-O bond. From the FT-IR spectra of polyaniline-MMT nanocomposite, it is shown that all the characteristic peaks of polyaniline are present and there is no specific change or shift of the polyaniline peaks in the polyaniline-MMT nanocomposite spectra, indicating that the incorporation of clay into polyaniline does not affect the chemical structure of polyaniline.

Figure 3 shows the UV–Vis absorption spectra for polyaniline and polyaniline-MMT nanocomposite coatings in pure NMP solvent obtained under galvanostatic conditions on the surface of 316L SS. The broad peak appearing at about 320 nm can be attributed to the π* transition in the benzeneoid ring of the polymer. The broad band around 655 nm can be attributed to the intramolecular transition between the benzeneoid and quinoid moieties in the polymer [48]. The UV–Vis absorption spectra of the polyaniline-MMT nanocomposite revealed a blue shift from the peak location for pure polyaniline, reflecting a decreased conjugated chain length of polyaniline in the polyaniline-MMT nanocomposite [48].

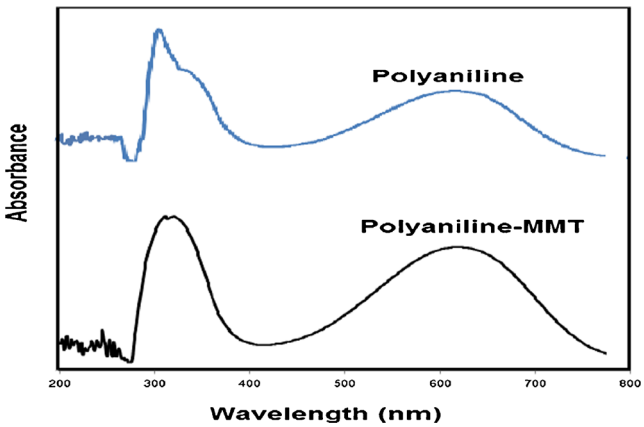

Fig. 3 UV–Vis spectra recorded for the electrosynthesized pure polyaniline and polyaniline-MMT nanocomposite on the 316L SS electrode

Figure 4a and b shows a high magnification SEM image from polyaniline and polyaniline-MMT nanocomposite coatings on 316L SS, respectively at current densities of the 0.75 mA cm^{-2}. Images show that the electropolymerized coatings are uniform and dense. The image b confirms the presence of MMT clay in coating matrix.

Corrosion protection performances of the electrosynthesized

The potentiodynamic polarization curves recorded in 0.5 M HCl medium for an uncoated 316L SS, polyaniline and polyaniline -MMT nanocomposite coated 316L SS are shown in Fig. 5a and b. The values of the E_{corr}, I_{corr}, polarization resistance (R_{pol}) and corrosion rate (CR) obtained from these curves are given in

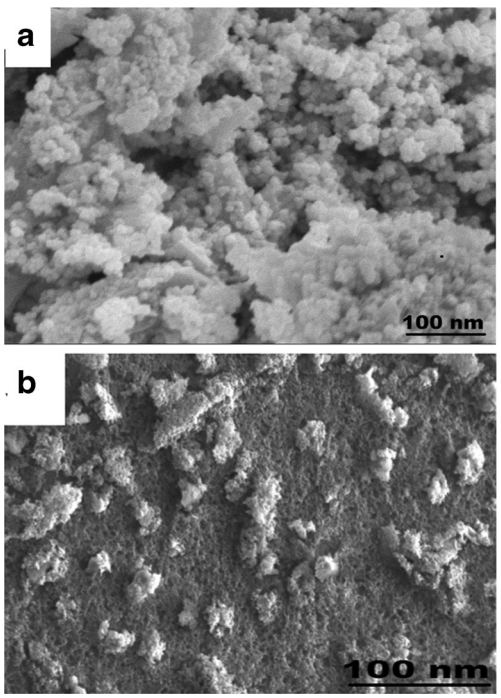

Fig. 4 SEM images of the coated 316L SS for 0.75 mA cm^{-2} **a** polyaniline coating and **b** polyaniline-MMT nanocomposite

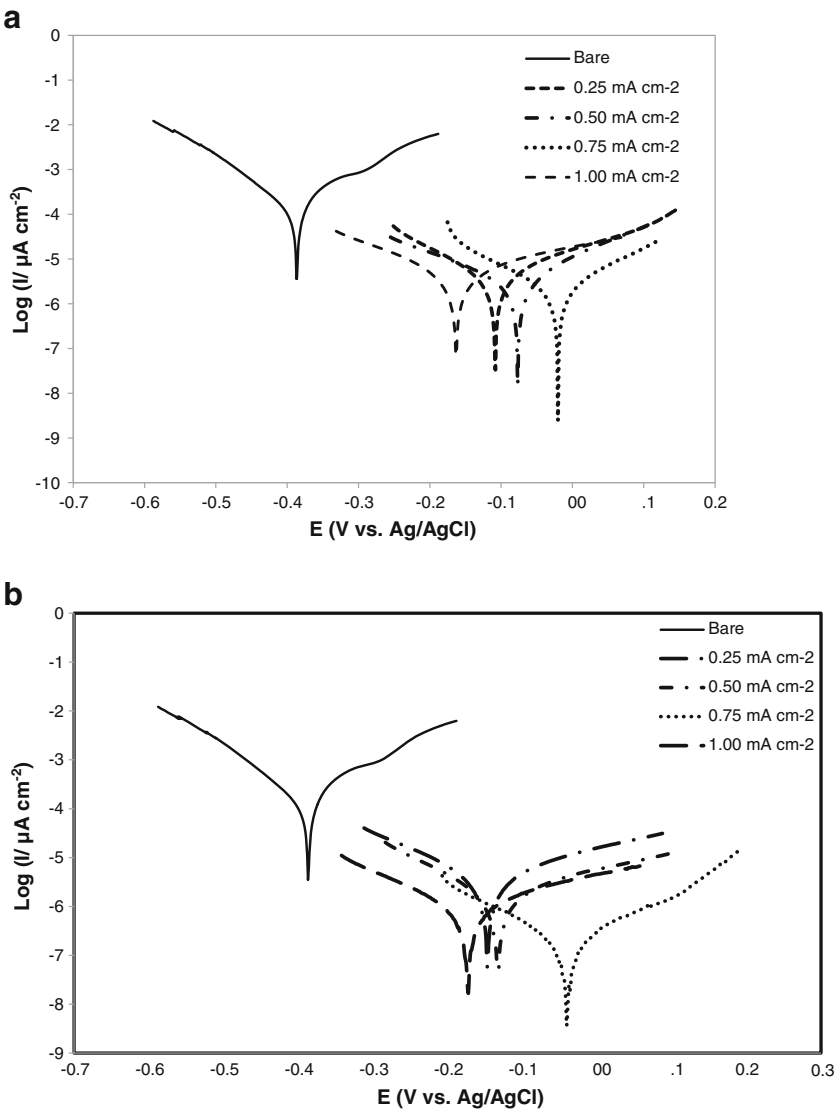

Fig. 5 Polarization behavior of electropolymerzied **a** polyaniline **b** polyaniline-MMT nanocomposite- coated on 316L SS at various current densities (mA cm^{-2}) in 0.5 M HCl medium

Table 1 Electrochemical parameters of electropolymerized polyaniline and polyaniline-MMT nanocomposite on 316L SS in 0.5 M HCl solution under the galvanostatic conditions at different current densities for 30 min

Coatings	Sample (mA cm^{-2})	*I*corr (µA cm^{-2})	*E*corr (mV)	*R*p (kΩ cm^2)	CR (mm $year^{-1}$)	*PE%*	*P%*
	Bare[a]	140.5	−0.386	0.124	1.63	–	–
polyaniline	0.25	5.75	−0.108	7.201	0.06	95.9	0.080
	0.50	4.90	−0.076	12.544	0.05	96.5	0.030
	0.75	3.48	−0.020	25.853	0.04	97.5	0.008
	1.00	9.73	−0.163	10.942	0.11	93.0	0.090
polyaniline-MMT	0.25	5.90	−0.146	9.263	0.080	95.7	0.094
	0.50	2.62	−0.132	19.445	0.030	98.1	0.040
	0.75	0.27	−0.040	136.021	0.003	99.8	0.002
	1.00	6.20	−0.172	35.912	0.072	95.5	0.033

(b_a: 0.21 V dec^{-1})[a]

Table 1. It was apparent that the current values of the coated sample are lower than that of the bare sample and corrosion potential of the coated sample is shifted to anodic direction. This result was pointed out the protective property of the coating against corrosive medium. From the measured corrosion current density values, the protection efficiency (*PE*) was obtained from the following equation [49]:

$$PE\% = \left[\left(I_{corr} - I_{corr(c)}\right)/I_{corr}\right] \times 100 \quad (1)$$

where I_{corr} and $I_{corr(c)}$ are the corrosion current density values in the absence and presence of polyaniline coating respectively.

The decrease in the I_{corr} was observed from 140.5 μA cm^{-2} for uncoated 316L SS to 3.48 and 0.27 μA cm^{-2} for polyaniline and polyaniline-MMT nanocomposite coatings respectively. The *CR* of polyaniline and polyaniline -MMT nanocomposite coated 316L SS are found to be 1.63, 0.04 and 0.003 mm $year^{-1}$, which are 41 and 540 times lower than that observed for uncoated 316L SS.

The polarization resistance (R_{pol}) is an important parameter, that ability of coating in prevention of electron exchange in a corrosive environment. As it can be seen in Table 1, R_{pol} increases from 0.124 kΩcm^2 for uncoated 316L SS to 25.853 and 136.021 kΩcm^2 for polyaniline and polyaniline-MMT nanocomposite coated 316L SS under optimal condition. These result that the coating of polyaniline-MMT nanocomposite is high polarization resistance.

It can be seen that the corrosion current of the polyaniline -MMT nanocomposite-coated was lower than and *PE*% is upper than polyaniline coated 316L SS. Therefore, it was found that the incorporation of MMT nanoparticles in the matrix coatings promotes the anticorrosive efficiency of the polyaniline -MMT nanocomposite coating on 316L SS. However, the enhanced corrosion protection by the polyaniline -MMT nanocomposite over the protection by the polyaniline might result from the nano layers of the MMT dispersed in the matrix coatings as filler that increase the tortuosity of the diffusion pathway of corrosive agents such as oxygen gas, hydrogen and chloride ions [48, 50].

The coating porosity is one of the important parameters, which strongly governs the anticorrosive behavior of the coatings. Therefore, measurement of the coating porosity is essential in order to estimate the overall corrosion resistance of the coated substrate. In this work, the porosity in polyaniline and polyaniline-MMT nanocomposite coatings on 316L SS substrates was determined from potentiodynamic polarization resistance measurements. The porosity in polymer coating was calculated using the relation [49]:

$$P = \left(R_{puc}/R_{pc}\right) \times 10^{-(|\Delta E|/ba)} \quad (2)$$

where *P* is the total porosity, R_{puc} the polarization resistance of the bare Cu, R_{pc} the measured polarization resistance of coated 316L SS, ΔE_{corr} the difference between corrosion potentials and b_a the anodic Tafel slope for bare 316L SS substrate. The porosity in polyaniline and polyaniline-MMT nanocomposite coatings (0.75 mA cm^{-2}) was found to be 0.008 and 0.002, respectively. As it can be seen, the porosity was decreased in presence of MMT.

In order to investigate the influence of the coating thickness on the porosity and corrosion protection properties of the polyaniline -MMT nanocomposite coatings, we have synthesized the coatings by various current densities and the potentiodynamic polarization resistance measurements were performed in an aqueous solution of in 0.5 M HCl medium. As can be seen from Table 1, the porosity in coatings does change significantly when the deposition current densities increases. This suggests that the thickness of the polyaniline and polyaniline -MMT nanocomposite coating may significantly influence the porosity in the coating. The lower values of the porosity in polyaniline and polyaniline-MMT nanocomposite coatings permit an improvement of the corrosion resistance by hindering the access of the electrolyte to the 316L SS substrates.

It seems that the electrode surface is gradually covered as the deposition current density is increased by initial layers of the coating and it continues while the surface of the electrode is fully covered. Then, the thickness of the coating increased as the deposition current density is more increased and therefore the efficiency of the coating decreased due to formation of the cracks and defects that are formed in the thickening stage at 1.00 mA cm^{-2}.

Therefore, the results obtained it can be concluded that in the much higher currents densities the polyaniline and polyaniline -MMT nanocomposite coated on 316L SS is high porosity, that cause increases the corrosion current and also, the PE% is reduced. According to the results, the optimum current density for the synthesis and investigation of the corrosion, current density of 0.75 mA cm^{-2}, which is covered in a uniform current density (low porosity) and enhanced corrosion resistance.

The corrosion behavior of polyaniline and polyaniline-MMT nanocomposite coated 316L SS in 0.5 M HCl medium has been found out by EIS methods. Figure 6a and b shows the Nyquist plot of impedance behavior of polyaniline and polyaniline -MMT nanocomposite coated 316L SS and these impedance plots were modeled by the equivalent circuit depicted in Fig. 7. The impedance parameters such as solution resistance (R_s), charge transfer resistance (R_{ct}) and double layer capacitance (C_{dl}) derived from these curves are given in Table 1. The Rct is the charge transfer resistance of the area at the metal/coating interface at which corrosion occurs and C_{dl} is the corresponding capacitance. Instead of capacitance, constant phase element

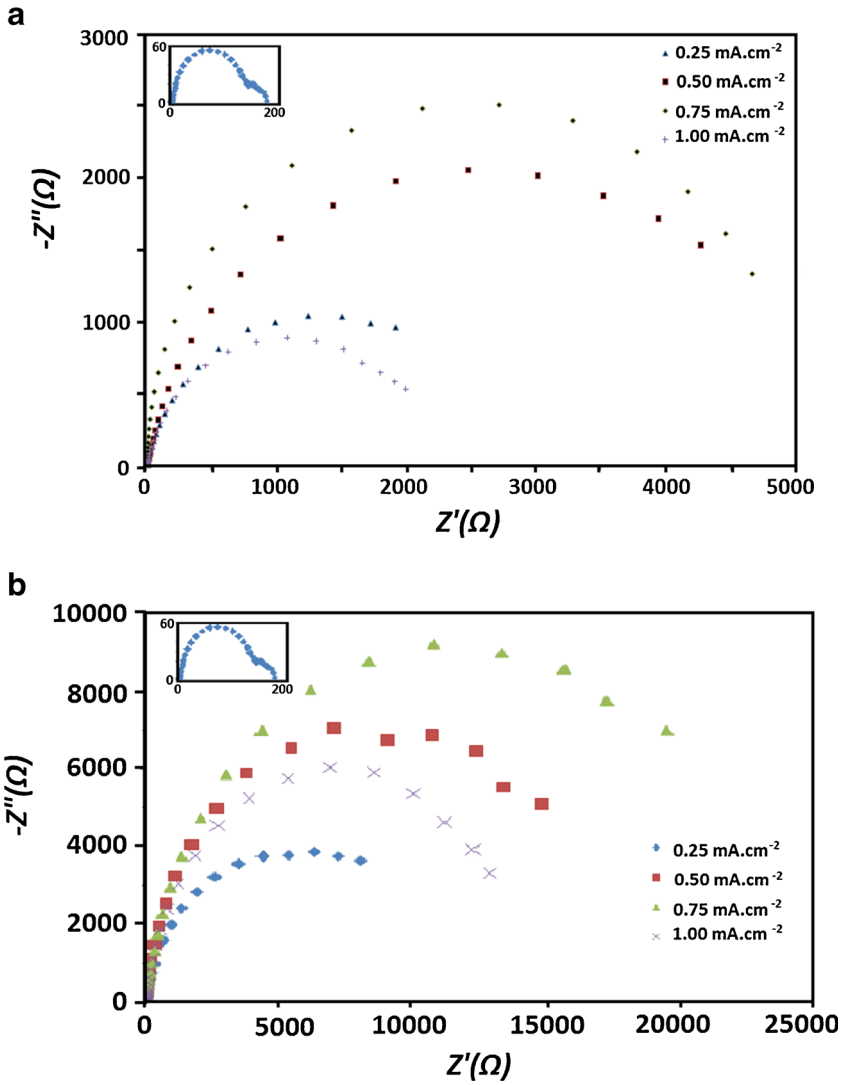

Fig. 6 Nyquist impedance plots for uncoated 316L SS and **a** polyaniline and **b** polyaniline-MMT nanocomposite coated 316L SS synthesized under galvanostatic conditions at various current densities (mA cm^{-2})

(*CPE*) was used. The *CPE* represents the deviation from the true capacitance behavior. For the description of a frequency independent phase shift between an applied alternating potential and its current response, a constant phase element (*CPE*) is used instead of capacitance (*C*). The CPE is defined by the mathematical expression [51, 52].

$$Z_{\mathrm{CPE}} = 1/Y_o(jw)^n$$

where Z_{CPE}, impedance of *CPE*; Y_0, a proportional factor; w, Angular frequency; j, $(-1)^{1/2}$; and n the exponential term,

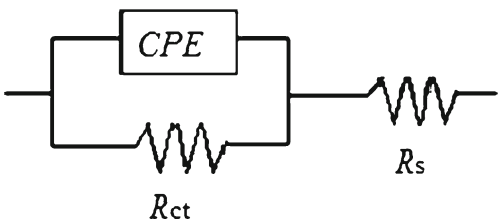

Fig. 7 Equivalent circuit model

which has many different explanations, it can be associated with the roughness of electrode surface [53], a distribution of reaction rates [52], non-uniform current distribution [54, 55], etc. The charge transfer resistance values of uncoated, polyaniline, polyaniline -MMT nanocomposite coated 316L SS in 0.5 M HCl are 0.13 kΩ cm^2, 5.04 kΩ cm^2 and 17.12 kΩcm^2 respectively under optimal condition. The percentage protection efficiency (*PE*) was calculated using the following equation [49]:

$$PE\% = \left[\left(R_{\mathrm{ct(c)}} - R_{\mathrm{ct}}\right)/R_{\mathrm{ct(c)}}\right] \times 100 \quad (3)$$

where R_{ct} and $R_{\mathrm{ct(c)}}$ are the charge transfer resistance in absence and presence of coating, respectively. These values show a protection efficiency of 97.3 % in the case of polyaniline -MMT nanocomposite coated 316L SS and 99.2 % protection efficiency in the case of polyaniline coated 316L SS. Besides, the coating capacitance values of polyaniline -MMT nanocomposite coated 316L SS is found to be very less which indicates the

Table 2 Impedance parameter values of the electrosynthesized polyaniline and polyaniline-MMT nanocomposite extracted from the fit to the equivalent circuit for the impedance spectra recorded in 0.5 M HCl medium

Coatings	Sample (mA cm^{-2})	R_s (Ω cm^2)	R_{ct} (kΩ cm^2)	C_{dl} (μF cm^{-2})	d^a (μm)	*PE%*
polyaniline	Bare	2.9	0.13	270.00	–	–
	0.25	3.27	1.90	57.01	0.65	92.8
	0.50	4.59	4.26	57.00	0.65	96.8
	0.75	4.46	5.04	56.08	0.66	97.3
	1.00	4.08	3.90	56.50	0.65	96.5
polyaniline-MMT	0.25	3.87	6.80	71.40	0.52	98.0
	0.50	3.92	13.60	70.00	0.53	99.0
	0.75	3.92	17.12	57.80	0.64	99.2
	1.00	3.53	12.01	69.20	0.53	98.8

[a] (ε_0=8.85×10^{-12} F/cm, ε=4.2, A=1 cm^2)

compact nature of the coating. Further, the double layer capacitance decreases in the case of polyaniline -MMT nanocomposite coated 316L SS which shows the reduced amount of iron dissolution reaction. These results show that MMT have improved the protective nature of polyaniline coating.

One of the important parameters for synthesis of the polymer coatings on the metal surface is calculating coating thickness which is an important feature for industrial applications. EIS data can be used for measurement of the thickness of polyaniline and polyaniline-MMT nanocomposite coatings. The polymer coating thickness on the surface of 316L SS by using of C_{dl} can be achieved according to the following equation [49]:

$$C_{dl} = \varepsilon_0 \varepsilon A/d \tag{4}$$

where ε is the dielectric constant of the environment, ε_0 is the vacuum permittivity, A is the electrode area and d is the thickness of the protective layer. According to Table 2, it can be concluded that the protection efficiency increased when coating thickness increased. On the other hand, these results

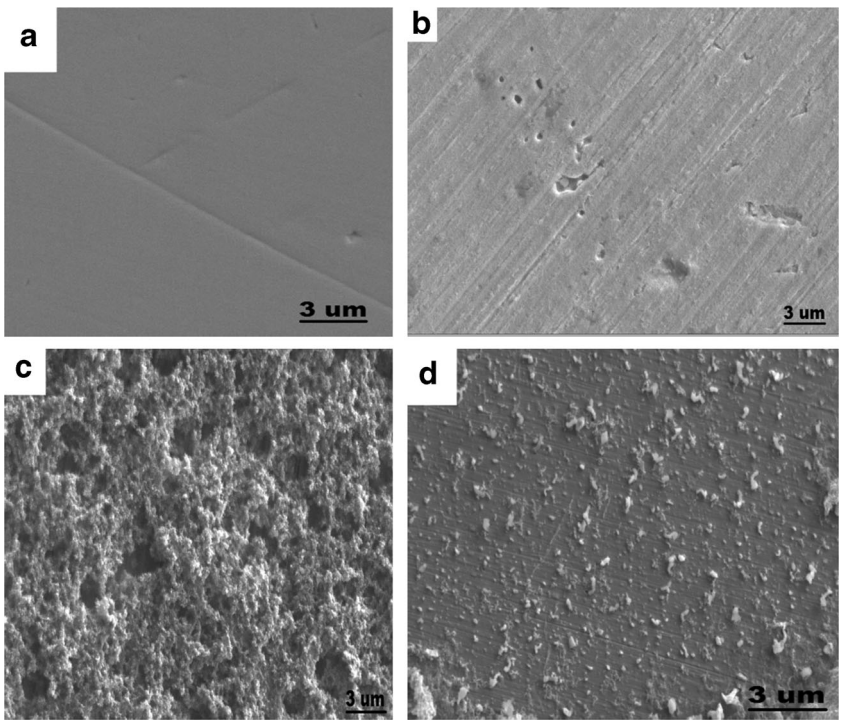

Fig. 8 SEM micrographs of abraded 316L SS (image **a**) pretreated 316L SS after corrosion (image **b**), polyaniline coating after corrosion (image **c**) and polyaniline-MMT nanocomposite coatings grown by an applied current density of 0.75 mA cm^{-2} after corrosion (image **d**)

show that the barrier properties of the coating on the 316L SS surface increased.

The *PE%* calculated from EIS data for polyaniline and polyaniline-MMT nanocomposite coated 316L SS respectively, which are in agreement with the potentiodynamic polarization results. It can be seen that the incorporation of MMT nanoparticles into the coating matrix exhibited better charge transfer resistances than polyaniline coated 316L SS electrodes. The effect of the nano-size additives improved the barrier properties of polymers for diffusion of solvent/gases. The increasing the area of synthesized electroactive polymer in the presence of nanoparticles can increase its ability to interact with the ions liberated during the corrosion reaction of 316L SS in the presence of HCl, water and oxygen [56, 57].

SEM characterization

The SEM images of abraded 316L SS (image a), pre-treated 316L SS after corrosion (image b), polyaniline coating after corrosion (image c) and polyaniline-MMT nanocomposite coating grown by an applied current density of 0.75 mA cm^{-2} after corrosion (image d) are shown in Fig. 8. Image b shows that numerous large pits and inequalities were formed after corrosion, which reveals severe damage on surface due to metal dissolution. Image c shows that the polyaniline coating was electrodeposited on the surface and protected it from the corrosion and image d shows that the polyaniline-MMT nanocomposite coating protects the 316L SS. It clearly reveals that the formed coatings on 316L SS surface are uniform and dense. The quality of the coatings is so excellent that no crack or detachment of the coatings is observed.

Conclusions

The polyaniline and polyaniline-MMT nanocomposite coatings were successfully direct electrosynthesized on 316L SS substrates from aqueous solution containing H_2SO_4 and aniline monomers with dispersed MMT nanoparticles for nanocomposite. Uniform compact and adherent coatings can be obtained under galvanostatic condition. Four various current densities of 0.25, 0.5, 0.75 and 1.00 mA cm^{-2} were applied for the formation of polyaniline and polyaniline-MMT nanocomposite coatings on 316L SS. The results showed that the current density of 0.75 mA cm^{-2} for the polymerization stage is the best condition for the synthesis of more compact and strongly adherent polyaniline and polyaniline-MMT nanocomposite coatings on 316L SS. The polyaniline and polyaniline-MMT nanocomposite coatings were characterized by FT-IR, UV–vis and SEM and the corrosion resistant properties of the electropolymerized coatings were evaluated using Tafel polarization and electrochemical impedance spectroscopy in 0.5 M HCl medium. The coating porosity was estimated by using the potentiodynamic polarization measurements and it was found that the porosity values are significantly lower for the polyaniline-MMT nanocomposite coatings as compared to the polyaniline. The EIS results are in good agreement with the potentiodynamic polarization measurements. This study reveals the polyaniline-MMT nanocomposite coating has excellent corrosion protection properties and can be considered as a potential coating material to protect 316L SS against corrosion in solution 0.5 M HCl. The enhanced corrosion protection effect of the polyaniline-MMT nanocomposite relative to polyaniline in the form of coating on metallic surface was attributed to the combination of the electrochemical property of the polyaniline and the barrier effect of the MMT nanoparticles dispersing in the composite. We believe that the coating helps to stabilize the passive film onto the substrate thus stopping the 316L SS corrosion.

Acknowledgments The authors are grateful to University of Kashan for supporting this work by Grant No (159194/7).

References

1. Gopi D, Govindaraju KM, Kavitha L, Basha KA (2011) Prog Org Coat 71:11–18
2. Shen GX, Chen YC, Lin CJ (2005) Thin Solid Films 489:130–136
3. Ganash AA, Al-Nowaiser FM, Al-Thabaiti SA, Hermas AA (2013) J Solid State Electrochem 17:849–860
4. Sathiyanarayanan S, Karpakam Kamaraj VK, Muthukrishnan S, Venkatachari G (2010) Surf Coat Technol 204:1426–1431
5. Sabirneeza AAF, Subhashini S (2013) J Appl Polym Sci 127:3084–3092
6. Negm NA, Ghuiba FM, Tawfik SM (2011) Corros Sci 53:3566–3575
7. Mansfeld F, Breslin CB, Pardo A, Perez FJ (1997) Surf Coat Technol 90:224–228
8. Ganash AA, Al-Nowaiser FM, Al-Thabaiti SA, Hermas AA (2011) Prog Org Coat 72:480–485
9. Tang YC, Katsuma S, Fujimoto S, Hiromoto S (2006) Acta Biomater 2:709–715
10. Okazaki Y, Gotoh E (2008) Corros Sci 50:3429–3438
11. Malik MA, Włodarczyk R, Kulesza PJ, Bala H, Miecznikowski K (2005) Corros Sci 47:771–783
12. Armelin E, Pla R, Lies F, Ramis X, Iribarren JI, Aleman C (2008) Corros Sci 50:721–728
13. Le DP, Yoo YH, Kim JG, Cho SM, Son YK (2009) Corros Sci 51: 330–338
14. DeBerry DW (1985) J Electrochem Soc 132:1022–1026
15. Kilmartin PA, Trier L, Wright GA (2002) Synth Met 131:99–109
16. Galkowski M, Malik MA, Kulesza PJ, Bala H, Miecznikowski K, Wlodarezyk R, Adamezyk L, Chojak M (2003) J Electrochem Soc 150:B249–B253
17. Gasparac R, Martin CR (2001) J Electrochem Soc 148:B138–B145
18. Wessling B (1994) Adv Mater 6:226–228
19. Cook A, Gabriel A, Laycoc NK (2004) J Electrochem Soc 151: B529–B535
20. Hermas AA, Nakayama M, Ogura K (2005) Electrochim Acta 50: 2001–2007
21. Hermas AA, Nakayama M, Ogura K (2005) Electrochim Acta 50: 3640–3647

22. Somani PR (2002) Mater Chem Phys 77:81–85
23. Ayad MM, Shenashin MA (2004) Eur Polymer J 40:197–202
24. Huang J, Moore JA, Acquaye JH, Kaner RB (2005) Macromolecules 38:317–321
25. Lim YS, Tan YP, Lim HN, Huang NM, Tan WT (2013) J Polym Res 20:156–164
26. Kraljic M, Mandic Z, Duic L (2003) Corrs Sci 45:181–189
27. Huh JH, Oh EJ, Cho JH (2005) Synth Met 153:13–16
28. Zhang T, Zeng CL (2005) Electrochim Acta 50:4721–47274
29. Alvial G, Matencio T, Neves BRA, Silva GG (2004) Electrochim Acta 49:3507–3516
30. Trabelsi W, Dhouibi L, Matoussi F, Triki E (2005) Synth Met 151: 19–24
31. Torres FG, Arroyo OH, Gomez C (2007) J Thermoplast Compos Mater 20:207–223
32. Vaisman J, Li L, Marom G, Kim JK (2007) Carbon 45:744–750
33. Cong H, Zhang J, Radosz M, Shen Y (2007) J Membr Sci 294:178–185
34. Geblinger N, Thiruvengadathan R, Regev O (2007) Compos Sci Technol 67:895–899
35. Schmidt D, Shah D, Giannelis EP (2006) Curr Opinion Solid State Mater Sci 6:205–212
36. Yu YH, Lin CY, Yeh JM, Lin WH (2003) Polymer 44:3553–3560
37. Malinauskas A, Malinauskiene J, Ramanavicius A (2005) Nanotechnology 16:R51–R62
38. Castagno KRL, Dalmoro V, Mauler RS, Azambuja DS (2010) J Polym Res 17:647–655
39. Hackman I, Hollaway L (2006) Compos Part A 37:1161–1170
40. Salavagione HJ, Diego CA, Selma T, Mohammed B, Abdelghani B, Emilia M (2008) Eur Polym J 44:1275–1284
41. Yeh JM, Liou SJ, Lai CY, Wu PC (2001) Chem Mater 13:1131–1136
42. Arora A, Choudhary V, Sharma DK (2011) J Polym Res 18:843–857
43. Kim JW, Liu F, Choi HJ, Hong SH, Joo JS (2003) Polymer 44:289–293
44. Yoshimoto S, Ohashi F, Ohnishi Y, Nonami T (2004) Synth Met 145: 265–270
45. Chang KC, Chen ST, Lin HF, Lin CY, Huang HH, Yeh JM, Yu YH (2008) Eur Polym J 44:13–23
46. Lai MC, Chang KC, Yeh JM, Liou SJ, Hsieh MF, Chang HS (2007) Eur Polym J 43:4219–4228
47. Yeh JM, Yao CT, Hsieh CF, Lin LH, Chen PL, JCh W, Yang HC, Wu CP (2008) Eur Polym J 44:3046–3056
48. Shabani-Nooshabadi M, Ghoreshi SM, Behpour M (2011) Corros Sci 53:3035–3042
49. Ghoreishi SM, Shabani-Nooshabadi M, Behpour M, Jafari Y (2012) Prog Org Coat 74:502–510
50. Tallman DE, Levine KL, Siripirom C, Gelling VC, Bierwagen GP, Croll SG (2008) Appl Surf Sci 254:5452–5459
51. Ashassi-Sorkhabi H, Seifzadeh D, Hosseini MG (2008) Corros Sci 50:3363–3370
52. Roeper DF, Chidambaram D, Clayton CR, Halada GP (2008) Electrochim Acta 53:2130–2134
53. Mulder WH, Sluyters JH, Pajkossy T, Nyikos L (1990) J Electroanal Chem 285:103–115
54. Kim CH, Pyun SI, Kim JH (2003) Electrochim Acta 48:3455–3463
55. Jorcin JB, Orazem ME, Pebere N, Tribollet B (2006) Electrochim Acta 51:1473–1479
56. Sathiyanarayanan S, SyedAzim S, Venkatachari G (2007) Electrochim Acta 52:2068–2074
57. Mahmoudian MR, Basirun WJ, Alias Y (2011) Appl Surf Sci 257: 3702–3708